ARTICLE

Quasi-classical Trajectory Study of the Intramolecular Isotope Effect in the Reaction $O(^3P)+H_2/HD$

Qiang Wei[a*], Xing Li[b], Tie Li[a]

a. Department of Applied Physics, Chongqing University of Technology, Chongqing 400050, China
b. School of Physics and Optoelectronic Technology, Dalian University of Technology, Dalian 116024, China

(Dated: Received on June 24, 2009; Accepted on September 10, 2009)

Theoretical studies of the dynamics of the reactions $O(^3P)+H_2/HD(v=0,\ j=0)\rightarrow OH+H$ have been performed with quasi-classical trajectory method (QCT) on an *ab initio* potential surface for the lowest triplet electronic state of $H_2O(^3A'')$. The QCT-calculated integral cross sections are in good agreement with the earlier time-dependent quantum mechanics results. The state-resolved rotational distributions reveal that the product OH rotational distributions for O+HD have a preference for populating highly internally excited states compared with the $O+H_2$ reaction. Distributions of differential cross sections show that directions of scattering are strongly dependent on the choice of quantum state. The polarization dependent generalized differential cross-sections and the distributions were calculated and a pronounced isotopic effect is revealed. The calculated results indicate that the product polarization is very sensitive to the mass factor.

Key words: Quasi-classical trajectory, Isotope effect, Alignment, Orientation

I. INTRODUCTION

The reaction $O(^3P)+H_2$ is of fundamental interest: it is one of the simplest hydrogen abstraction reactions, which is important in many combustion processes. The reaction and its isotopic variants have received considerable attention both theoretically [1−11] and experimentally [12]. Especially, Han and coworkers first introduced the nonadiabatic quantum wave packet approach to study nonadiabatic reaction dynamics and they presented for the first time an exact quantum study of spin-orbit-induced intersystem crossing effects in the title reaction [1]. Braunstein *et al.* [6] and Balakrishnan [7,8] have reported their dynamics calculations on the $O(^3P)+H_2\rightarrow OH+H$ reaction and the agreement between these calculated total reaction cross sections and the experimental results have been found. For the isotopic reaction $O(^3P)+HD$, Song *et al.* has proved that the major contribution to the isotopic effect comes from reorientation of HD as O atom approaches [9]. Gordon *et al* examined all hydrogen isotope effects and reported experimental measurements of k_{HD}/k_{DH} using laser-induced fluorescence techniques as well as found very strong negative temperature dependence for the kinetic isotope effect (KIE) [10,11].

However, the previous work in reaction dynamics has only focused on scalar properties. Complete information on the forces acting in the reaction also requires a consideration of vector properties, as they are key indicators of the anisotropy of the potential energy surface involved in the reaction [13−15]. Hence, a complete understanding of the gas-phase reaction dynamics is only possible after considering both scalar and vector properties together [16−18]. One aspect of this polarization is the correlation between reactant and product relative velocity vectors, the $\mathbf{k}$-$\mathbf{k}'$-$\mathbf{j}'$ correlation, which provides information otherwise lost by averaging over the random azimuthal orientation of impact parameters [19]. To shed more light on the state-to-state dynamics, in this work, we primarily explore the polarization of product rotational angular momentum in the reaction and vector correlations whether found to be very sensitive to isotopic substitute.

II. COMPUTATION METHODS

A. Rotational polarization of the product

In the center-of-mass (CM) frame shown in Fig.1, the reagent relative velocity vector $\mathbf{k}$ is parallel to the z-axis. The x-z plane is the scattering plane containing the initial and final relative velocity vectors, $\mathbf{k}$ and $\mathbf{k}'$. θ_t is the angle between the reagent relative velocity and product relative velocity, namely, scattering angle. θ_r and ϕ_r are the polar and azimuthal angles of the final rotational momentum $\mathbf{j}'$. The distribution function

*Author to whom correspondence should be addressed. E-mail: qiangwei2004@yahoo.cn, FAX: +86-23-62563055

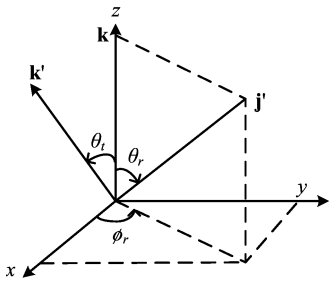

FIG. 1 The center-of-mass coordinate system used to describe the **k**, **k**′, and **j**′ distribution.

$P(\theta_r)$ describing the **k**-**j**′ correlation can be expanded in a series of Legendre polynomials as [15,16,20,21]:

$$P(\theta_r) = \frac{1}{2}\sum_k (2k+1) {a_0}^k P_k(\cos\theta_r) \tag{1}$$

$${a_0}^k = \langle P_k(\cos\theta_r)\rangle \tag{2}$$

The expanding coefficients ${a_0}^k$ are called the orientation (k is odd) and the alignment (k is even) parameter. k=2 indicate the product rotational alignment [13,14]:

$$\begin{aligned} {a_0}^2 &= \langle P_2(\cos\theta_r)\rangle \\ &= \langle P_2(j'k)\rangle \\ &= \frac{1}{2}\left\langle 3\cos^2\theta_r - 1\right\rangle \end{aligned} \tag{3}$$

The dihedral angle distribution function $P(\phi_r)$ describing the **k**-**k**′-**j**′ correlation expanded in a Fourier series [15,16,20,21]:

$$P(\phi_r) = \frac{1}{2\pi}\left[1 + \sum_{n(\text{even})\geq 2} a_n\cos(n\phi_r) + \sum_{n(\text{odd})\geq 1} b_n\sin\phi_r\right] \tag{4}$$

$$a_n = 2\left\langle\cos(n\phi_r)\right\rangle, \quad b_n = 2\left\langle\sin(n\phi_r)\right\rangle \tag{5}$$

The full three-dimensional angular distribution associated with **k**-**k**′-**j**′ can be represented by a set of generalized polarization-dependent differential cross-sections (PDDCSs) in the CM frame that is described in [20−22]. The fully correlated CM angular distribution is written as the sum

$$P(\omega_t,\omega_r) = \sum_{kq}\frac{[k]}{4\pi}\frac{1}{\sigma}\frac{\mathrm{d}\sigma_{kq}}{\mathrm{d}\omega_t}C_{kq}(\theta_r,\phi_r) \tag{6}$$

where $[k]$=2k+1, $(1/\sigma)(\mathrm{d}\sigma_{kq}/\mathrm{d}\omega_t)$ is a generalized PDDCS, and $C_{kq}(\theta_r,\phi_r)$ are modified spherical harmonics [20−22]. The differential cross-section is given by

$$\begin{aligned} \frac{1}{\sigma}\frac{\mathrm{d}\sigma_{00}}{\mathrm{d}\omega_t} &= P(\omega_t) \\ &= \sum_{k_1}\frac{[k_1]}{4\pi}[k_1]h_0^{k_1}(k_1,0)P_{k_1}(\cos\theta_t) \end{aligned} \tag{7}$$

The bipolar moments $h_0^{k_1}(k_1,0)$ are evaluated using the expectation values of the Legendre moments of the differential cross-section,

$$\begin{aligned} S_{00}^{k_1} &= h_0^{k_1}(k_1,0) \\ &= \langle P_{k_1}(\cos\theta_t)\rangle \end{aligned} \tag{8}$$

The remaining PDDCS with k=2, q=0, 1, and 2, namely, $(2\pi/\sigma)(\mathrm{d}\sigma_{2,0}/\mathrm{d}\omega_t)$, $(2\pi/\sigma)(\mathrm{d}\sigma_{2,1-}/\mathrm{d}\omega_t)$, and $(2\pi/\sigma)(\mathrm{d}\sigma_{2,2+}/\mathrm{d}\omega_t)$.

B. Potential energy surface and quasi-classical trajectory calculations

In this calculation, BMS1 potential energy surface [24] has been employed. The BMS1 PES for the O(^{3}P)+H_2 system in the lowest $^3A''$ state is built using *ab initio* data calculated by Rogers *et al.* [23] and the double many-body expansion formalism. To obtain a better description of the long range interactions, a semi-empirical representation of the long-range van der Waals force has been considered. The reaction barrier is 0.569 eV above the O(^{3}P)+H_2 asymptote limit and a van der Waals minimum (−0.02 eV) is found at a collinear reactant configuration ($C_{\infty v}$) with the O atom at 6.2a_0 from the H_2 center of mass.

The quasi-classical trajectory calculations are standard [21,22,25] and the quasi-classical trajectory method (QCT) stereodynamics code used in this calculation was provided by Professor Ke-li Han. The QCT calculations have been performed for the collision energy range of 0.5−1.1 eV, with sixth order simplectic integration [25] by running batches of 5×10^4 trajectories. The integration step size is chosen as 0.1 fs and the trajectories are started at an initial distance of 10 Å between the O atom and the centre of the mass of the H_2 or HD molecule. The initial azimuthal orientation angle and polar angle of the reagent molecule internuclear axis are randomly sampled using Monte Carlo method.

III. RESULTS AND DISCUSSION

A. Cross sections and rotational state distributions of the product

The total cross sections for the reaction O(^{3}P)+H_2(v=0, j=0)→OH+H are shown in Fig.2. We compare our results with the time-dependent quantum mechanics (TDQM) calculations [26]. The QCT results

DOI:10.1088/1674-0068/22/05/523-528

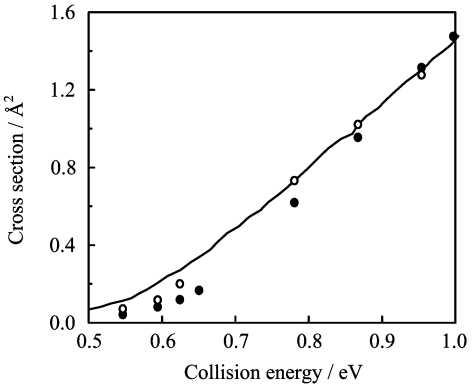

FIG. 2 Cross sections for the O(^{3}P)+H_2/HD(v=0,j=0) →OH+H reaction as functions of the collision energy. Filled circles: QCT results of O+H_2; open circles: QCT results of O+HD; solid curve: TDQM data of Ref.[26].

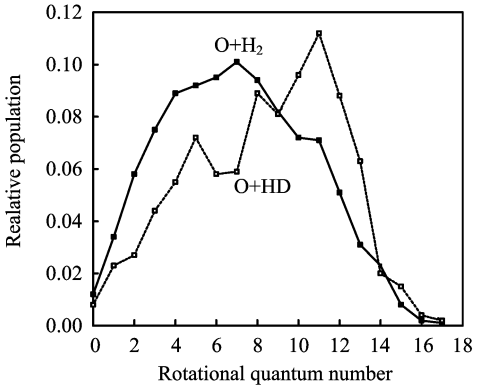

FIG. 3 Comparison between the QCT-calculated rotational distribution of the product OH(v'=0) molecule for O(^{3}P)+H_2 and that for O(^{3}P)+HD reactions at a collision energy of 0.87 eV.

(filled circles) and TDQM (open circles line) calculation [26] are obtained with BMS1 PES, which is a single fitted *ab initio* surface for the lowest $H_2O(^3A'')$ state. As expected [25], the QCT results are in excellent agreement with the quantum result at high collision energies ($E_{\rm coll}\geq$0.85 eV). However, near the threshold energy, the quantum cross sections are significantly higher than those calculated using classical mechanics. We believe the differences between the TDQM and present QCT cross sections arise from differences between quantum and classical mechanics. The quantum results are much more adiabatic [6], which proceeds along the reaction path with constant internal vibrational energy and becomes sensitive to these effective energy thresholds. As the collision complex is formed, the quantized energy associated with bound motions added to the minimum energy path creates effective energy thresholds for reaction.

Other potentially significant quantum effects such as tunneling appear to be significant at low collision energies. As the collision energy becomes much larger than the barrier heights, these effects should diminish, which is what we observe.

For O+HD(v=0, j=0) the cross sections for producing OH and OD have been added together. The major difference is that O+HD is more reactive than O+H_2 at energies $E_{\rm coll}\leq$0.85 eV. As can be seen that isotopic substitution for the energy surface results in some changes of reaction mechanism, such as barrier heights. For O+H_2 reaction the effective barrier height is 0.568 eV [26] and for O+HD it is 0.534 eV. We believe that the smaller effective barrier height gives rise to larger reactive probability.

Figure 3 shows a comparison of the QCT-calculated rotational distribution of the product OH(v'=0) molecule for O+H_2 reaction with the same product for the O+HD reaction at a collision energy of 0.87 eV. The product OH rotational distributions for O+HD have a preference for populating highly internally excited states compared with the O+H_2 reaction. In previous work [27], the rotational distributions are related to repulsive forces between the H atoms during decay of the reaction complex. For the O(^{3}P)+H_2/HD reactions, we get the product rotational energy for O+H_2 is $E'_{\rm rot}$=0.162 eV while $E'_{\rm rot}$=0.184 eV for O+HD. Repulsive forces energy of HD molecular is larger and transfers to product rotational energy $E'_{\rm rot}$ more effectively, which results in populating highly internally excitation.

The present QCT calculation was carried out without considering the role of the nonadiabatic effect [1,28,29] in the scattering process.

B. Product polarization

The distributions of $P(\theta_r)$ and $P(\phi_r)$ calculated on BMS1 PES at the collision energy of 0.87 eV for the reactions O(^{3}P)+H_2/HD(v=0,j=0)→OH+H/D are presented in Fig.4. The $P(\theta_r)$ distributions, describing the **k**-**j**′ correlation, peak at θ_r angles close to 90° and are symmetric with respect to 90° because of the planar symmetry of the system. It is clear that there is an obvious discrepancy between the distribution of $P(\theta_r)$ of the two reactions. The peak of $P(\theta_r)$ distribution of the reaction O+H_2 is much higher than that of the reaction O+HD, which indicates that the degree of alignment of OH from the reaction O+H_2 is different from that of HD from the reaction O+HD. A simple way to express the degree of product rotational polarization is through the center-of-mass frame alignment parameter $\langle P_2(j'k)\rangle$. The value of $\langle P_2(j'k)\rangle$ on the BMS1 PES is −0.428 for O+H_2 reaction, while it is −0.405 for O+HD reaction, which imply that the product rotational alignment effects become weaker with the increase of the atomic mass. The difference of the $P(\theta_r)$ distribution is probably attributed to the difference of

DOI:10.1088/1674-0068/22/05/523-528

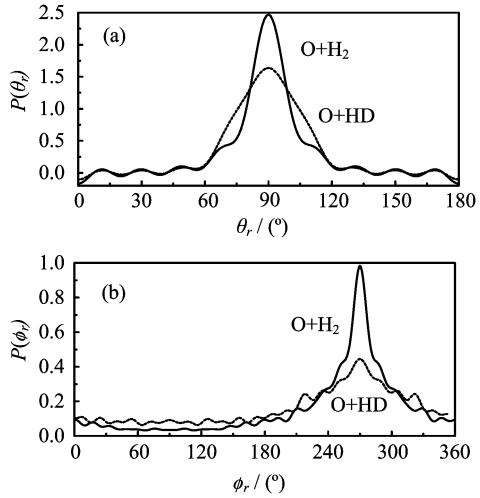

FIG. 4 Rotational polarization of the OH product from the $O(^3P)+H_2/HD(v=0,\ j=0)\rightarrow OH+H$ reactions at a collision energy of 0.87 eV. (a) Distribution of $P(\theta_r)$, reflecting the **k**-**j**′ correlation. (b) Dihedral angle distribution of **j**′, $P(\phi_r)$, with respect to the **k**-**k**′ plane.

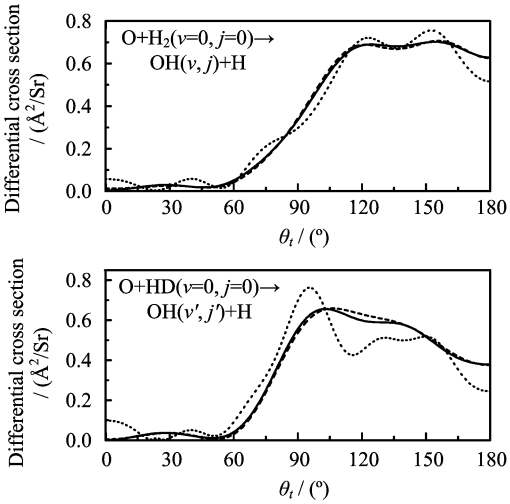

FIG. 5 Differential cross sections for the $O(^3P)+H_2/HD$ $(v=0,\ j=0)\rightarrow OH+H/D$ reactions at a collision energy of 0.87 eV. The solid line shows data for the average, the dash line shows data for OH ($v'=0$), and the dot line shows data for OH ($v'=1$).

mass factor (*i.e.*, $\cos^2\beta=m_Am_C/[(m_A+m_B)(m_B+m_C)]$ for the reaction A+BC→AB+C) between the reaction $O+H_2$ ($\cos^2\beta=0.444$) and the reaction O+HD ($\cos^2\beta=0.593$). An increase of mass factor $\cos^2\beta$ will reduce the anisotropic distribution of the product rotational angular momentum j', which is consistent with experimental observation [17].

The dihedral angle distribution $P(\phi_r)$, describing the **k**-**k**′-**j**′ correlations, are shown in Fig.4(b). These $P(\phi_r)$ distributions tend to be asymmetric with respect to the **k**-**k**′ scattering plane, directly reflecting the strong polarization of product rotational angular momentum. The peaks at ϕ_r angles close to 270° indicate a preference for left-handed product rotation in planes parallel to the scattering plane. We use the term "in-plane" to refer to this preference of product molecule rotating in planes parallel to the scattering plane, and the term "out-of-plane" to refer to the preference of product molecule rotating in planes perpendicular to the scattering plane at the same time. At the collision energy of 0.87 eV, for the $O+H_2$ reaction, the peak in the $P(\phi_r)$ distributions at ϕ_r angles close to 270° but almost disappear at ϕ_r=90°, which implies the rotational angular momentum vector of the product OH is mainly aligned along the negative direction of y-axis of the CM frame. For the O+HD reaction, the peak at 270° becomes lower, which implies that the product rotational alignment effect is weaker. However, the breadth of the peak is almost invariant, which indicates that a preference of in-plane reaction mechanism has little changed. As mentioned above, the distribution of the product angular momentum vector is sensitive to the mass factor. During the reactive encounter, total angular momentum is conserved, **j**+**L**=**j**′+**L**′ (here **L** and **L**′ are the reagent and product orbital angular momentum). According to the impulse model [30], the larger product atom will take more angular momentum away and reduces the anisotropic distribution of **j**′.

Figure 5 show a comparison of the differential cross sections (DCSs) for the reactions $O+H_2$ and O+HD on the BSM1 PES. The DCSs only describe the **k**-**k**′ correlation or the scattering direction of the product and is not associated with the orientation and alignment of the product rotational angular momentum vector j'. The solid lines in the figures represent the average DCSs. It can be seen that OH product molecules from the reaction $O+H_2$ are backward scattered while OH molecules from the reaction O+HD present a preference for sideward scattered.

As shown in Fig.5, because of the high probabilities, for both the reactions, the DCSs for $v'=0$ (dash line) is close to the average which provides major contribution to directions of scattering. For initial reagents $v=0$, the distributions of final products OH vibrational states mostly center on $v'=0$, which is the same as Ref.[31]. The branching ratio $OH(v'=0)/OH(v'=1)$ is 3.574 for $O+H_2$ reaction closed to the value ∼3.67 from Ref.[22]. The results show the vibrational population in the product is more or less a copy of the vibrational structure in the reagents. It is interesting that, for $v'=1$, the products of O+HD reaction represent sideward scattering more notably. Based on previous works [6] for this system, we believe that the directions of scattering are strongly dependent on the choice of quantum state.

Figure 6 present PDDCS $(2\pi/\sigma)(d\sigma_{2,0}/d\omega_t)$, PDDCS $(2\pi/\sigma)(d\sigma_{2,1-}/d\omega_t)$, and PDDCS $(2\pi/\sigma)(d\sigma_{2,2+}/d\omega_t)$, respectively. The PDDCS $(2\pi/\sigma)(d\sigma_{2,0}/d\omega_t)$ is the ex-

DOI:10.1088/1674-0068/22/05/523-528

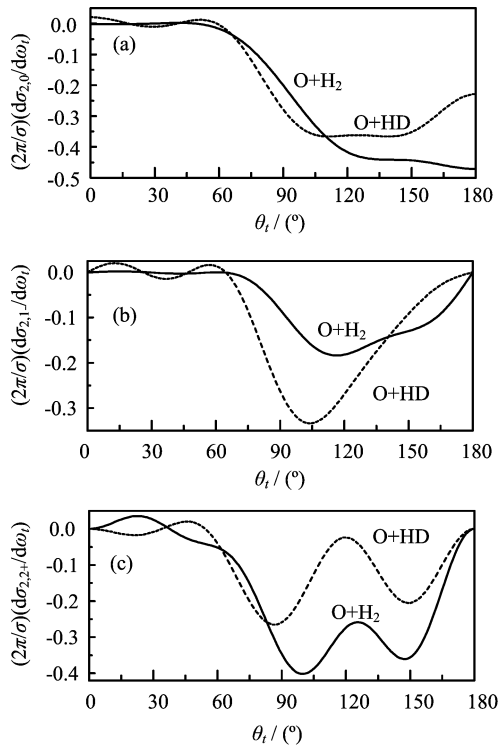

FIG. 6 PDDCSs for the O(^{3}P)+H_2/HD(v=0, j=0)→ OH+H/D reactions at acollision energy of 0.87 eV. (a) The PDDCS with (k,q)=(2,0). (b) The PDDCS with (k,q)=(2,1−). (c) The PDDCS with (k,q)=(2,2+).

pectation value of the second Legendre moment. The behavior of $(2\pi/\sigma)(\mathrm{d}\sigma_{2,0}/\mathrm{d}\omega_t)$ shows the trend opposite to that of $(2\pi/\sigma)(\mathrm{d}\sigma_{00}/\mathrm{d}\omega_t)$, which indicates that $\mathbf{j}'$ is strongly aligned perpendicular to k. These results show that the $(2\pi/\sigma)(\mathrm{d}\sigma_{2,0}/\mathrm{d}\omega_t)$ is related to alignment moment $\langle P_2(j'k)\rangle$. The calculated values of the product rotational alignment parameter $\langle P_2(j'k)\rangle$ are −0.428 and −0.405 corresponding to O+H_2→OH+H and O+HD→OH+D reactions and thus the product rotational alignment for O+H_2 is stronger than O+HD. This is in consistence with the product alignment prediction from the $P(\theta_r)$ distribution shown in Fig.3(a). The distribution of $(2\pi/\sigma)(\mathrm{d}\sigma_{2,0}/\mathrm{d}\omega_t)$ of the reaction O+H_2 differs from that of the reaction O+HD when θ_t is larger than 60°. For θ_t<60°, the polarization trend of both reactions is consistent. As discussed in Ref.[13,14], the difference of the distribution of $(2\pi/\sigma)(\mathrm{d}\sigma_{2,0}/\mathrm{d}\omega_t)$ between the two reactions may come from the difference of the mass factor ($\cos^2\beta$=0.444 for O+H_2 and $\cos^2\beta$=0.593 for O+HD) between the two reactions.

It can also be seen in Fig.6 (b) and (c) that the PDDCSs with $q\neq0$ are zero at the extremities of forward and backward scattering. At these limiting scattering angles, the $\mathbf{k}$-$\mathbf{k}'$ scattering plane is not determined and the value of these PDDCSs with $q\neq0$ must be zero [20]. The distributions of $(2\pi/\sigma)(\mathrm{d}\sigma_{2,1-}/\mathrm{d}\omega_t)$, which are related to $\langle-\sin 2\theta_r\cos\phi_r\rangle$, are depicted in Fig.6(b). It can be seen in that there is significant difference between the two reactions. The values of $(2\pi/\sigma)(\mathrm{d}\sigma_{2,1-}/\mathrm{d}\omega_t)$ of OH, for O+H_2 reaction, are negative at all scattering angles, which indicate the product OH molecules are aligned along the direction of vector $\mathbf{x}$+$\mathbf{z}$, while the values are positive at the range of scattering angles 0°−25° and 45°−65°and are negative at other scattering angles, which shows that the product alignment OH is along the direction of vector both $\mathbf{x}-\mathbf{z}$ and $\mathbf{x}+\mathbf{z}$. The strongest polarizations of the products of the two reactions are at about 105° and 115°, respectively.

Figure 6(c) shows the PDDCS $(2\pi/\sigma)(\mathrm{d}\sigma_{2,2+}/\mathrm{d}\omega_t)$ distribution, which is relative to $\langle\sin^2\theta_r\cos 2\phi_r\rangle$, and the values of $(2\pi/\sigma)(\mathrm{d}\sigma_{2,2+}/\mathrm{d}\omega_t)$ are negative for all scattering angles, which indicates the remarkable preference of product alignment along y-axis. The product of the O+H_2 reaction displays a strongest polarization at about 100°, and the strongest polarization for O+HD is at about 90°. In addition, the value of $(2\pi/\sigma)(\mathrm{d}\sigma_{2,2+}/\mathrm{d}\omega_t)$ for O+H_2 reaction is more negative than for O+HD reaction, for all but the forward direction, which indicates that the products from O+H_2 reaction are more aligned.

IV. CONCLUSION

In this work, we presented a quasi-classical trajectory dynamic study for the reactions O(^{3}P)+H_2/HD(v=0, j=0)→OH+H/D on the BMS1 potential energy surface. The integral cross sections, state-resolved rotational distributions, and product polarization were calculated for a collision energy range from 0.5 eV to 1.1 eV. The QCT-calculated integral cross sections are in good agreement with earlier TDQM results. The state-resolved rotational distributions in v'=0 at a collision of 0.87 eV show clearly that the product OH rotational distributions for O+HD have a preference for populating highly internally excited states. At the product-state-resolved level, the DCSs for the two reactions were plotted and the results reveal that the directions of scattering are strongly dependent on the choice of quantum state. The PDDCSs $(2\pi/\sigma)(\mathrm{d}\sigma_{2,0}/\mathrm{d}\omega_t)$, $(2\pi/\sigma)(\mathrm{d}\sigma_{2,1-}/\mathrm{d}\omega_t)$, $(2\pi/\sigma)(\mathrm{d}\sigma_{2,2+}/\mathrm{d}\omega_t)$ and the distribution of $P(\theta_r)$, $P(\phi_r)$ have been calculated. The product rotational angular momentum vectors j' of the products from the two reactions are not only aligned, but also oriented. Calculations also show that, on BMS1 PES, the product polarization is very sensitive to the mass factor $\cos^2\beta$. For the reactions O(^{3}P)+H_2/HD, an increase of mass factor can reduce the anisotropic distribution of the product rotational angular momentum j'.

V. ACKNOWLEDGEMENT

This work was supported by the Chongqing University of Technology (No.01-60-32).

DOI:10.1088/1674-0068/22/05/523-528

[1] T. S. Chu, X. Zhang, and K. L. Han, J. Chem. Phys. **122**, 214301 (2005).
[2] G. C. Schatz, A. F. Wagner, S. P. Walch, and J. M. Bowman, J. Chem. Phys. **74**, 4984 (1981).
[3] K. T. Lee, J. M. Bowman, A. F. Wagner, and G. C. Schatz, J. Chem. Phys. **76**, 3653 (1982).
[4] J. M. Bowman and A. F. Wagner, J. Chem. Phys. **86**, 1967 (1987).
[5] N. Cohen and K. R. Westberg, J. Phys. Chem. Ref. Data **12**, 531 (1983).
[6] M. Braunstein, S. Adler-Golden, B. Maiti, and G. C. Schatz, J. Chem. Phys. **120**, 4316 (2004).
[7] N. Balakrishnan, J. Chem. Phys. **121**, 6346 (2004).
[8] P. F. Weck and N. Balakrishnan, J. Chem. Phys. **123**, 144308 (2005).
[9] J. B. Song and E. A. Gislason, J. Chem. Phys. **99**, 5117 (1993).
[10] B. C. Garrett, D. G. Truhlar, J. M. Bowman, A. F. Wagner, D. Robie, S. Arepalli, N. Presser, and R. J. Gordon, J. Am. Chem. Soc. **108**, 3515 (1986).
[11] D. C. Robie, S. Arepalli, N. Presser, T. Kitsopoulos, and R. J. Gordon, J. Chem. Phys. **92**, 7382 (1990).
[12] D. J. Garton, T. K. Minton, B. Maiti, D. Troya, and G. C. Schatz, J. Chem. Phys. **118**, 1585 (2003).
[13] M. L. Wang, K. L. Han, and G. Z. He, J. Chem. Phys. **109**, 5446 (1998).
[14] M. L. Wang, K. L. Han, and G. Z. He, J. Phys. Chem. A **102**, 20204 (1998).
[15] M. D. Chen, K. L. Han, and N. Q. Lou, J. Chem. Phys. **118**, 4463 (2003).
[16] M. Gonzalez, J. D. Sierra, R. Francia, and R. Sayos, J. Phys. Chem. A **101**, 8 (1997).
[17] R. J. Li, K. L. Han, F. E. Li, R. C. Lu, G. Z. He, and N. Q. Lou, Chem. Phys. Lett. **220**, 281 (1994).
[18] M. D. Chen, B. Y. Tang, K. L. Han, and N. Q. Lou, Chem. Phys. Lett. **337**, 349 (2001).
[19] J. D. Barnwell, J. G. Loeser, and D. R. Herschbach, J. Phys. Chem. **87**, 6 (1983).
[20] M. Brouard, H. Lambert, S. P. Rayner, and J. P. Simons, Mol. Phys. **89**, 403 (1996).
[21] L. P. Ju, K. L. Han, and J. Z. H. Zhang, J. Comput. Chem. **30**, 305 (2009).
[22] M. D. Chen, B. Y. Tang, K. L. Han, and N. Q. Lou, Chin. J. Chem. Phys. **15**, 247 (2002).
[23] S. Rogers, D. Wang, A. Kuppermann, and S. Walch, J. Phys. Chem. A **104**, 2308 (2000).
[24] J. Brandão, C. Mogo, and B. C. Silva, J. Chem. Phys. **121**, 8861 (2004).
[25] X. Zhang and K. L. Han, Int. J. Quant. Chem. **106**, 1815 (2006).
[26] W. L. Wang, C. Rosa, and J. Brandão, Chem. Phys. Lett. **418**, 250 (2006).
[27] M. S. Fitzcharles and G. C. Schatz, J. Phys. Chem. **90**, 16 (1986).
[28] T. S. Chu, Y. Zhang, and K. L. Han, Int. Rev. Phys. Chem. **25**, 201 (2006).
[29] T. S. Chu and K. L. Han, Phys. Chem. Chem. Phys. **10**, 2431 (2008).
[30] K. L. Han, G. Z. He, and N. Q. Lou, Chin. J. Chem. Phys. **2**, 323 (1989).
[31] R. Schinke and W. A. Lester Jr., J. Chem. Phys. **70**, 11 (1979).

DOI:10.1088/1674-0068/22/05/523-528